

Graphene Oxide-hybridized Waterborne Epoxy Coating for Simultaneous Anticorrosive and Antibiofilm Functions

Ying Zhou ^{1,2}, Haoran Wang ⁴, Cheng Zhang ⁴, Qixin Zhou ^{4*}, Debora F Rodrigues ^{2,3*}

¹ Department of Materials Chemistry, Huzhou University, Huzhou 313000, P. R. China

² Department of Civil and Environmental Engineering, University of Houston, Houston, TX 77204-5003, United States

³ Department of Material Science and Engineering, University of Houston, Houston, TX 77204-4003, U.S.A.

⁴ Department of Chemical, Biomolecular, and Corrosion Engineering, The University of Akron, 264 Wolf Ledges Parkway, Akron, Ohio, 44325, United States

***Corresponding author:** dfrigirodrigues@uh.edu, phone: +1-713-743-149

qzhou@uakron.edu, phone: +1-330-972-7159

Abstract:

Multifunctional coatings with simultaneous antibacterial and anticorrosive properties are essential for marine environments, oil & gas industry, medical settings, and domestic/public appliances to preserve integrity and functionality of pipes, instruments, and surfaces. In this work, we developed a simple and effective method to prepare **graphene oxide** (GO) hybridized waterborne epoxy (GOWE) coating to simultaneously improve anticorrosive and **antibacterial** properties. The effects of different GO filler **ratios (0.05, 0.1, 0.5, 1 wt.%)** on the electrochemical and **antibacterial** behaviors of the waterborne epoxy coating were investigated **over short- and long-term periods**. The **electrochemical behavior was analyzed with salt solution for 64 days**. The **antibacterial effect of GOWE coating was evaluated with *Shewanella oneidensis* (MR-1)**, which is a microorganism that **can be involved in corrosion**. Our results revealed that concentrations as low as 0.5 wt.% of the GO was effective for superior anticorrosive and **antibacterial** performance than the waterborne epoxy coating without Graphene oxide. This result is due to the high

hydrophilicity of the Graphene oxide fillers, which allowed great dispersion in the waterborne epoxy coating matrix. Furthermore, this study used a corrosion relevant bacterium as a model organism, *i.e.*, *Shewanella oneidensis* (MR-1), which is more relevant for real word applications. This as-prepared GO-hybridized waterborne polymeric hybrid film provides new insight into the application of 2D nanomaterial polymer composites for simultaneous anticorrosive and antibacterial applications.

Key words: Anticorrosive coating, Antibacterial coating, Graphene Oxide, Waterborne Epoxy Coating.

1. Introduction

Metals or alloys are widely used materials in industry and in our daily life, however they are prone to electrochemical corrosion and biofilm-formation, which can impact their performance^{1,2}. The global economic loss of biofilm and corrosion is enormous, which is estimated to be 2.5 trillion (3.4% of the global GDP)³⁻⁵. Additionally, there is urgent health concerns involving increased chances of infection caused by various bacterial biofilms, especially in medical facilities⁶. To prevent such issues, special surface modifications involving antibacterial and anticorrosion properties are required for long term applications of these metallic materials in industrial facilities (e.g. oil & gas equipment⁷ and marine industry⁸), biomedical implants (e.g. bone/tissue implants^{9,10}), and domestic appliances¹¹. Hence, both anticorrosive and antibacterial coatings must be developed for these metallic surfaces.

Epoxy is an efficient coating material and is commonly used to enhance the interfacial surface property due to its strong adhesion, excellent corrosion resistance, low curing shrinkage, good reservoir for additive corrosion inhibitors, and outstanding chemical properties ¹²⁻¹⁴. However, the main drawback of epoxy coatings is their tendency to suffer from surface abrasion resulting in localized defects and corrosion, and the potential polymer degradation under UV radiation ¹⁵. Therefore, recent studies have been conducted to incorporate inorganic fillers in the epoxy matrix to stimulate a synergic effect and overcome these challenges. For instance, inorganic particles, like montmorillonite, was shown to provide good barrier effect and enhance the bonding strength at the surface interface. However, there are still some issues with the incorporation of these inorganic fillers, such as complex manufacturing, high dosage, or easy cracking ^{16,17}.

More recently, nano-sized fillers (like SiO₂, TiO₂, ZnO) have been studied to alleviate microscopic defects and enhance the crosslinking density of the coating due to their high specific surface area ¹⁸. Among the nanofillers, **graphene oxide** (GO), as a relatively new class of materials for corrosion control¹⁹, has been considered as an ideal candidate for real potential large scale applications due to its outstanding properties, including mechanical, electrical, low cost, aqueous/thermal stability, barrier effect, high specific surface area (~2630 m²/g), and inherent antibacterial property ¹⁹⁻²¹. Researchers have shown great interest in Graphene oxide or Graphene oxide derivative composites for anticorrosive protection ^{22,23}.

Furthermore, researchers have also found that Graphene oxide composite polymeric coatings are promising antibacterial materials due to its ability to induce oxidative stress

by reactive oxygen species (ROS)³. For instance, Liu et al.²⁴ have reported that a solvent-borne epoxy with GO exhibited high antibacterial capability against *E.coli*. Graphene oxide has also shown to improve the antibacterial property of other polymers (e.g., poly DMA, poly (DMA-co-MEA)) in our previous studies^{25,26}. Additionally, graphene/GO and their derivatives have even exhibited a potential effect against COVID-19²⁷.

Recently, modification of waterborne polymeric coatings with Graphene oxide and its derivatives was exploited for specific functions and barrier performance enhancement, including antibacterial and anticorrosive properties^{28,29}. This interest arise from the increasing pressure for low carbon emission requirements, where waterborne polymers have been considered as a promising coating material with negligible VOC emission^{30,31}. More recently, Graphene oxide or their derivatives have been incorporated into waterborne polymeric matrix coatings, such as waterborne epoxy (WEP) and waterborne polyurethane (WPU) for simultaneous anticorrosive and antibacterial properties³². However, most of the studies used *Escherichia coli* (*E. coli*) as their model organism, which is not involved in corrosive activity. Herein, in our study, to simulate the actual steel corrosion environment, a Fe (III) reduction bacterium (IRB) model, *Shewanella oneidensis* MR-1, which can contribute to steel corrosion³³, was applied to systematically investigate the antibacterial function for potential real applications.

Specifically, the objectives of this study are to systematically investigate the doping concentration of Graphene oxide on the corrosion resistance of GOWE coating through a long-term electrochemical testing and to determine the antibacterial property of GOWE towards *Shewanella oneidensis* biofilm formation for both short-term and extended periods

using confocal laser scanning microscopy (CLSM) analysis. The materials produced were fully characterized to determine the dispersion of the **Graphene oxide** nanofiller in the WEP matrix as well as the successful formation of GOWE films through optic spectra, Raman, and field emission scanning electron microscopy (FESEM) analysis. Our research presents an effective strategy to produce a GOWE coating with simultaneous anticorrosive property and **antibacterial** function, with the potential for further applications in industrial, medical, and domestic fields.

2. Experimental

2.1. Materials

Waterborne epoxy resin (BECKOPOX EP 385W) and polyamine curing agent (BECKOPOX EH 613W) were obtained from Allnex Company (Langley, SC, USA). Luria-Bertani (LB) broth medium were purchased from Fisher-Scientific (Massachusetts, USA). Graphite (< 20 μm), sulfuric acid (H_2SO_4 , 98 wt. %), sodium nitrate, potassium permanganate, and hydrogen peroxide (30 wt.%) were purchased from Sigma Aldrich (Austin, TX, USA). Propidium iodide (PI) and SYTO9 dyes were obtained from Invitrogen Corporation (CA, USA). All reagents and solvents were used without further purification. All the chemicals were ACS grade.

2.2. Preparation of **Graphene oxide** nanoplates

Graphene oxide nanofiller was synthesized from natural graphite flakes using the modified Hummer's method, which was reported in our previous study ³⁴. Briefly, 2.5 g of graphite, 25 mL of concentrated H_2SO_4 , and 2.0 g of KMnO_4 were mixed in an ice bath and followed by stirring at 35 °C for 10 h. Then the mixture was further heated at 90 ± 1

°C for 1.5 h with drop wise dosing of H₂O₂ solution. Finally, the **Graphene oxide** suspension was centrifuged at 8000 rpm and washed 4-5 times with distilled water. The washed samples were further freeze-dried to achieve the final product.

2.3. Graphene oxide-water epoxy composite (GOWE) coating fabrication

Concentrations (wt.%) of 0.05, 0.1, 0.5, and 1 **Graphene oxide** were first dispersed in the waterborne epoxy resin by ultrasonic treatment for 1 h in an ice bath. Subsequently, a stoichiometric amount of polyamine curing agent was added to the dispersion. The above mixture was magnetically stirred for 20 min, followed by sonication for 15 min to remove air bubbles. Then the coating mixture was applied onto a steel substrate (QD36, Q-Lab Corporation, Ohio, US) to prepare GOWE coatings. The prepared coatings were left at room temperature for 24 h, followed by thermally curing at 120 °C for 1 h. The film preparation procedure is shown in Figure 1. The dry film thickness of the control (without adding **Graphene oxide**) and GOWE coatings were around 60 µm measured by a thickness gauge (byko-test 8500, BYK). The formulation of the waterborne epoxy coating with **Graphene oxide** nanofillers is shown in Table 1.

Table 1. Formulation of **graphene oxide** hybridized waterborne epoxy coating.

GO (mg)	Waterborne epoxy resin (Solid content: 56 wt.%)	Curing agent (Solid content: 80 wt.%)	Dry thickness (μm)
	(g)	(g)	
GOWE-0	0	5	0.79
GOWE-0.05	1.72	5	0.79
GOWE-0.1	3.43	5	0.79
GOWE-0.5	17.16	5	0.79
GOWE-1	34.32	5	0.79

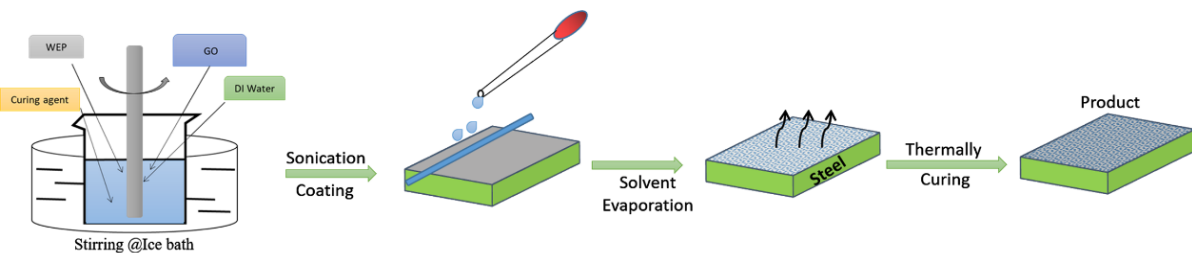


Figure 1. Schematic illustration of the GOWE coating preparation.

2.4. Corrosive resistance measurement

The corrosion resistance of coated samples was measured through electrochemical impedance spectroscopy (EIS) measurements by using the Reference 600+ Potentiostat (Gamry Instrument). The testing coatings were immersed in 3.5 wt.% NaCl solution with an exposure area of 7.07 cm^2 . The steel panel, saturated calomel electrode (SCE), and platinum mesh with 6.25 cm^2 surface area were used as working, reference, and counter

electrodes, respectively. All EIS tests were run in a Faraday cage at room temperature using 10 mV AC perturbation with a frequency range of $10^5\text{--}10^2$ Hz.

For the biofilm testing, the coating samples were cut into 2×2 cm small coupons. The backside and the edges of the coating coupons were applied with epoxy coating to avoid water penetration. The coating coupons after the biofilm testing were immersed in 3.5 wt.% NaCl solution for corrosion resistance assay.

2.5. Antibacterial performance testing

Antibacterial experiments were performed using a model metal reduction bacterium (*S. oneidensis* MR-1, Gram negative). *S. oneidensis* MR-1 was cultured overnight in a freshly prepared Luria-Bertani broth medium (LB, 1.0 wt.% tryptone, 0.5 wt.% yeast extract, 1.0 wt. % NaCl, 1.5 wt.% agar powder) with constant shaking (150 rpm, 30 °C) by using a shaker (Thermo Fisher, U.S.A.). The pH of the medium was adjusted to 7.0. The initial concentration of bacteria in the LB media was in the range of $\sim 3.0\times10^7$ CFU/mL ($OD_{600} = 0.60$). The details of the microbial biofilm growth were described in our previous study ^{3,35}. Briefly, bacterial growth was batch cultivated in a sterile 6-well plate (BioLite, U.S.) at 28 °C in LB medium. Before transferring to the plates, each coated steel plate was sterilized with UV light for 15 min in the biosafety hood. After that, 100 µl of the *S. oneidensis* culture was dosed to 10 mL of LB growth media. Then 100 µl of the above diluted culture mixture plus 6 mL of LB medium were transferred to six sterilized steel plates. The plates were further incubated at 30 °C for short term (72 h) and long term (10 days) under static conditions. For the long-term test, the *S. oneidensis* culture medium was replaced with 2 mL fresh media each day. After the testing, the specimens were gently rinsed three times with Phosphate Buffered Saline (PBS) to remove nonadherent bacteria

for further characterization³. All the testing were performed in triplicate and repeated at least three times for analysis.

2.6. Characterization and analysis

All coupons coated with the GOWE for corrosion and biofilm growth were characterized using Fourier transformed infrared spectroscopy, Raman spectroscopy, Scanning Electron microscopy (SEM) and confocal microscopy. The spectra were obtained with the Nicolet iS10 FT-IR Spectrometer (resolution: 4 cm⁻¹; scan number: 32) equipped with Nicolet smart attenuated total reflectance. The range of scanning wavenumber was from 4000 to 400 cm⁻¹. The Raman measurements were conducted to analyze the elemental composition using a Czerny-Turner Raman microspectroscopy (IHR320, HORIBA Scientific). The analysis was done with an excitation wavelength of 532 nm. The field emission SEM (Tescan Lyra3) was used for capturing the structural morphology of the coated samples.

A confocal laser scanning microscope (CLSM, Leica Lasertechnik, Heidelberg, Germany) was used to investigate the distribution of living and dead cells on the coating interface. For the confocal imaging, the coating samples were removed from the liquid culture under a biosafety hood. The biofilms were stained with a live/dead backlight bacterial viability kit (Invitrogen)¹². This kit contains two nucleic acid dyes: SYTO 9 and propidium iodide (PI)²⁵. The detailed procedure of the biofilm formation quantification is described in our previous study³. All analyses were done in triplicate.

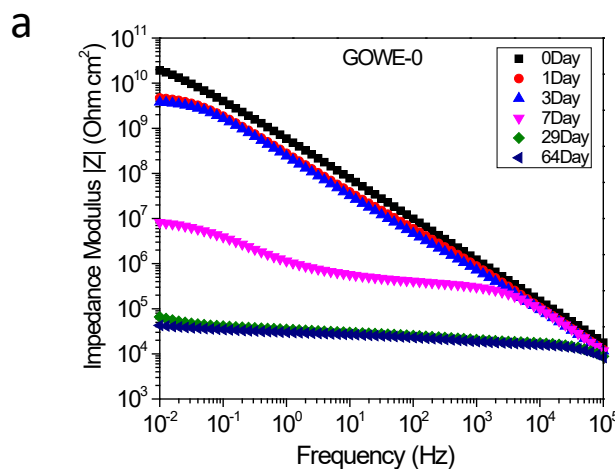
3. Results and discussion

3.1. Anticorrosive property of GOWE coating

Before electrochemical impedance measurements, the open circuit potential (OCP) was measured to achieve a steady potential. In this study, the OCP value of Graphene oxide hybrid coating (GOWE-0.1) was higher than the pure epoxy coating sample (data not shown), which indicated the barrier role of Graphene oxide nanofiller in the epoxy matrix.

EIS measurements were performed to semi-quantitatively evaluate the overall anticorrosive properties of the developed GO-hybridized composite coatings with different nano doping ratio at various immersion periods (0 day to 64 days in 3.5 wt.% NaCl solution). The Bode plots of $\log |Z|$ vs $\log f$ for the prepared coatings are shown in Figure 2. The initial measurements showed that the impedance modulus at 0.01 Hz of all the coatings was larger than 10^{10} Ohm·cm², which indicated an excellent corrosion protection³⁶. All the GOWE coatings maintained a much higher initial impedance modulus at 0.01Hz ($\sim 10^{11}$ Ohm·cm²) (Figure 2b) than the pure epoxy coating ($\sim 10^{10}$ Ohm·cm²), which revealed that generally the graphene oxide nanofiller could significantly improve the inherent corrosion resistance of waterborne epoxy coatings. On the other hand, during the long-term immersion time in the saline solution, due to the diffusion of water and corrosion ions into the coating substrates³⁷, both GOWE and pure epoxy coatings showed a decreasing trend of impedance modulus at 0.01 Hz. This phenomenon was more evident for the pure waterborne epoxy coatings, since the impedance modulus of GOWE-0 at low frequency region reduced sharply with longer immersion time. The result shows a steep degradation of impedance modulus, which dropped about six orders of magnitude (1.90×10^{10} Ohm·cm² to 6.5×10^4 Ohm·cm²) in 29 days of immersion, then remained stable for 64 days (Figure 2a).

In contrast, for GOWE-0.05 and GOWE-0.1 coatings, the impedance modulus at 0.01Hz showed a much slower degradation trend as compared to the other coatings and maintained a value of up to 9.0×10^9 Ohm·cm² and 9.7×10^9 Ohm·cm² after 64 days of immersion, which corresponded to two and one orders of magnitude decline for GOWE-0.05 and GOWE-0.1, respectively. The results suggested that the Graphene oxide nanofiller could effectively prevent corrosion. However, interestingly, with the increasing of GO doping ratio, GOWE-0.5 and GOWE-1 coatings exhibited a higher initial low-frequency impedance modulus but they dropped three and four orders of magnitude, respectively, after 64 days of immersion. This drop could be the result of the aggregation of 2D Graphene oxide nanosheets in the coating, and thus some local “defects” were generated during the coating curing process, which deteriorated the barrier capability of the coatings³⁸. This phenomenon was further confirmed via SEM imaging (Figure 2b). As a result, the concentrations of 0.1 wt.% Graphene oxide presented the best corrosion resistance than the other Graphene oxide concentrations. These results illustrated that well-dispersed Graphene oxide can effectively enhance the barrier properties of anti-corrosion coatings.



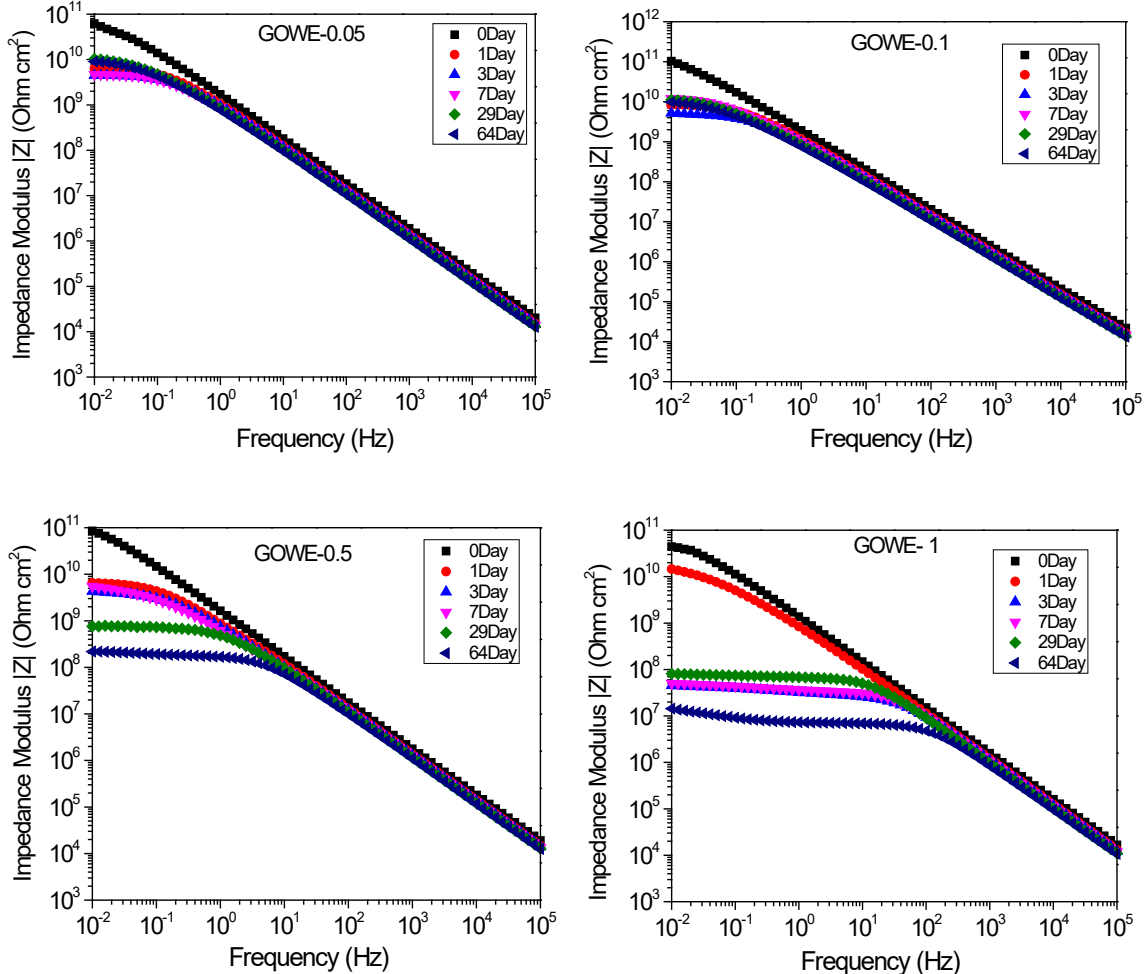
b

Figure 2. (a) Bode plots of neat waterborne epoxy coating GOWE-0 (without **Graphene oxide**) in the immersion of 3.5 wt.% NaCl solution; and (b) Bode plots of GOWE coatings (GOWE-0.05, GOWE-0.1, GOWE-0.5, GOWE-1) in the immersion of 3.5 wt.% NaCl solution. The formulation of GOWE coatings is listed in Table 1.

Furthermore, from the SEM characterization of the coatings, the GOWE-0.1 coating film exhibited the best **Graphene oxide** dispersion within the epoxy matrix, presenting a more homogeneous and smooth coating surface without significant defects or clusters (Figure 3b). The GOWE-0.5 (0.5 wt.% GO) (Figure 3c), on the other hand, showed obvious

defects on the coated surface, which came from the heterogenous dispersion of **Graphene oxide** in the epoxy matrix when the **graphene oxide** content was high.

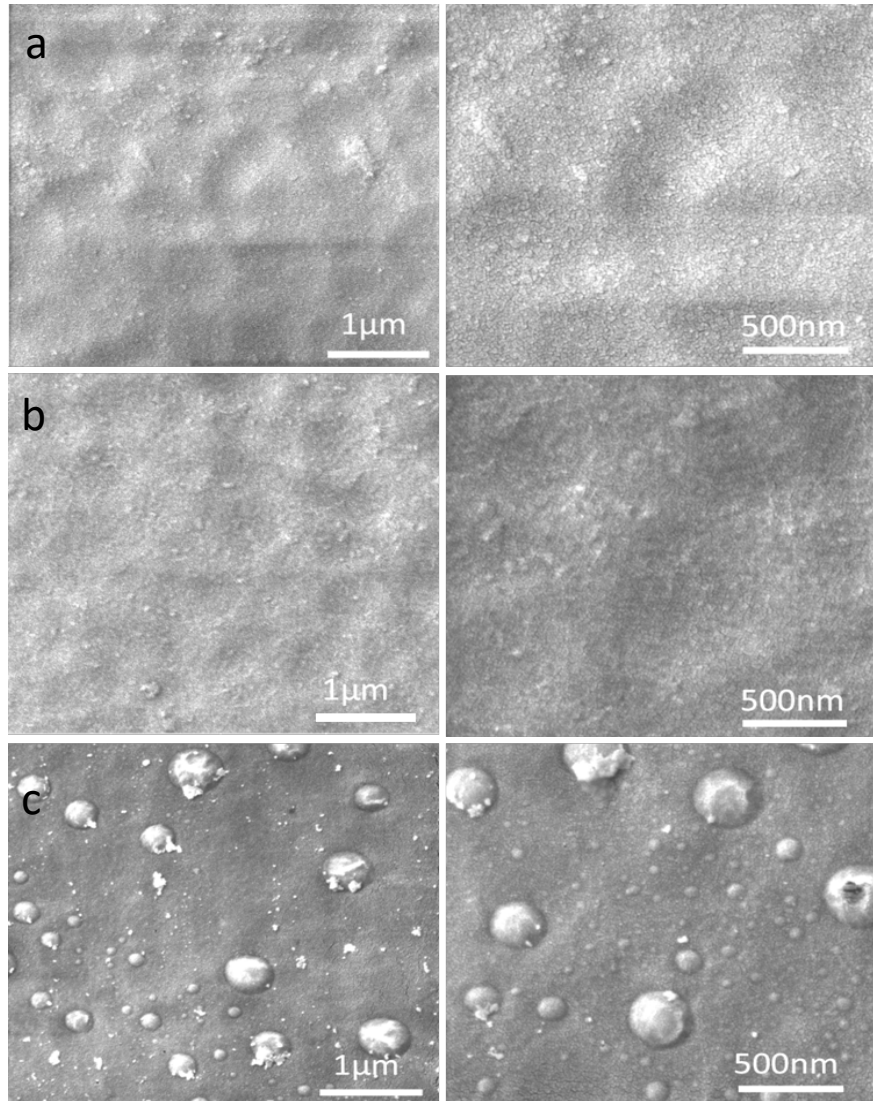


Figure 3. SEM images of the coatings a) WEP (control, without **Graphene oxide**), b) GOWE-0.1 (0.1 wt.% **Graphene oxide**) and c) GOWE-0.5 (0.5 wt.% **Graphene oxide**).

3.2. Antibacterial property of GOWE coatings

3.2.1. Effects of **Graphene oxide** concentration on biofilm formation

The growth of *S. oneidensis* on the coated surface was monitored to determine the antibacterial performance of the GOWE coatings. *S. oneidensis* growth mainly includes the process of initial attachment, cells rapid division on the surface, and isolated microcolonies formation. Eventually biofilms will develop into an extensive **three-dimensional** structure with strong interactions with the surface due to electrostatic, Van der Waals, and hydrophobic forces ^{39,40}.

The analysis of the biofilm formed on the GOWE coatings was done via the live-dead staining and observation through **confocal microscopy**. In this work, the waterborne epoxy films (control) and GOWE films with different **Graphene oxide** concentrations (0.05 wt.%, 0.1 wt.%, 0.5 wt.%, 1 wt.%) were exposed to the culture of *S. oneidensis* *MR-1* in LB growth medium (containing 1 wt.% NaCl) overnight to simulate a real environmental condition. As illustrated in Figure 4, the CLSM images for the surfaces of the control coating (without GO) and the bare steel coupon were almost completely green **and had a thick biofilm** after 72 h exposure, which demonstrated that a healthy biofilm was formed on these surfaces. In contrast, an overwhelming fraction of dead cells were observed on the surfaces of GOWE coating films, which demonstrated that **Graphene oxide** had a high ability to inhibit bacterial growth (see supporting information). When **Graphene oxide** content increased from 0.05 wt.% (Figure 4c) to 0.5 wt.% (Figure 4e), less biofilm was observed on the coated surfaces. However, as the GO concentration increased to 1 wt.% (Figure 4f), **the antibacterial capacity reduced as seen from the increasing numbers of live cells (green) on the coated surface. The less uniform biofilm growth 1 wt.% Graphene oxide loading could be due to Graphene oxide aggregation and subsequent random distribution in the coating.** Considering the results of the salt corrosion above and the

antimicrobial experiments, the 0.1 wt.% Graphene oxide concentration was considered the optimal dosage for the coating for simultaneous antibacterial and anticorrosion properties.

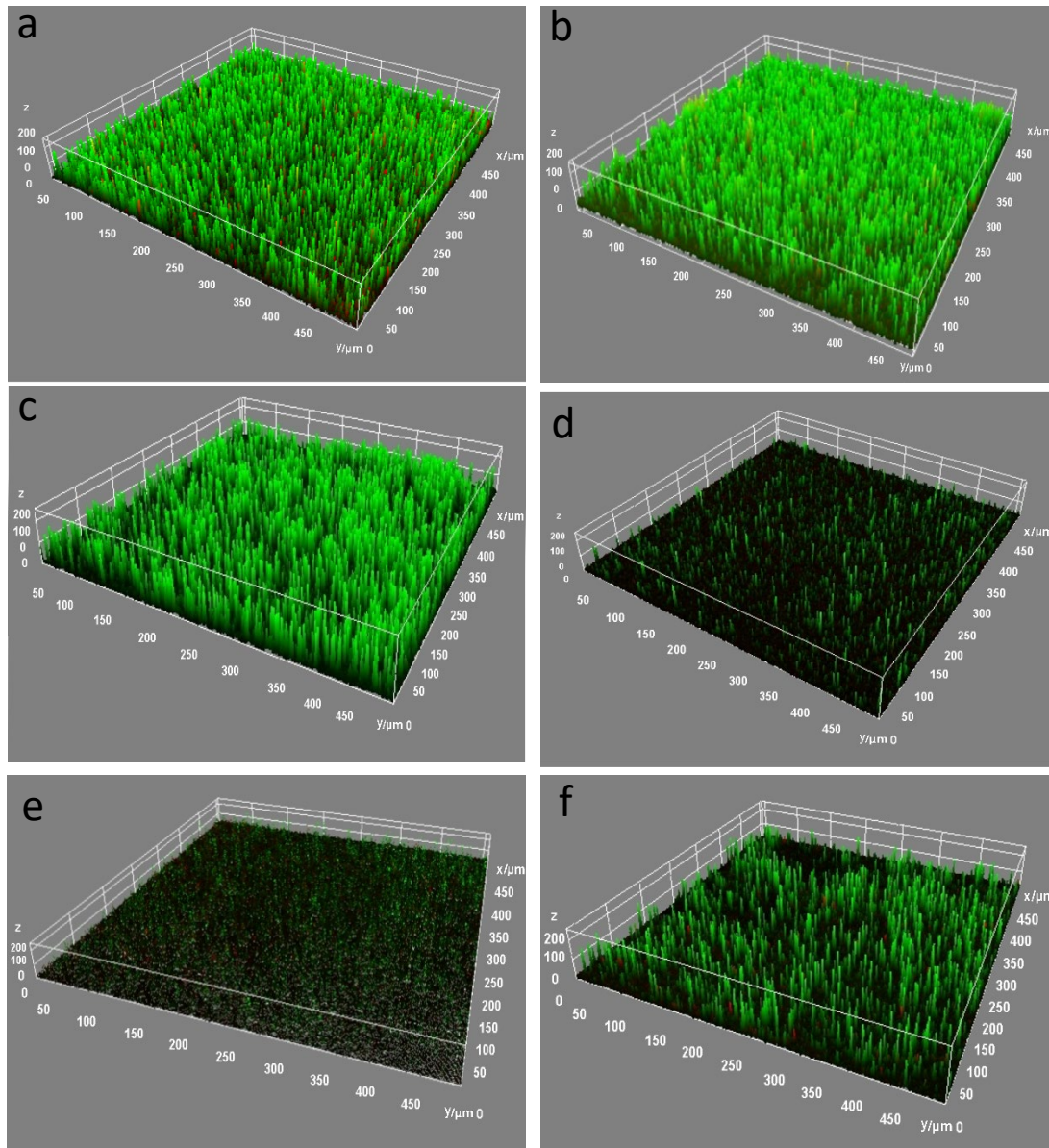


Figure 4. CLSM images of biofilms growth for 72 h on different coating surfaces. a) bare steel; b) WEP coating (control); c) GOWE-0.05 (0.05 wt.% GO); d) GOWE-0.1 (0.1 wt.% GO); e) GOWE-0.5 (0.5 wt.% GO); f) GOWE-1(1 wt.% GO). The green color corresponds to living bacterial cells growing on the surface. Experiments were run at 25 °C under static batch condition. The units are in micron.

3.2.2. Long-term antibacterial performance

In this investigation, the above optimized GOWE-0.1 coating was selected for the long-term exposure investigation of *S. oneidensis* MR-1 in LB growth medium to evaluate the coating antibacterial performance. As shown in Figure 5a, most of the *S. oneidensis* cells were alive (green) with almost no dead (red) cells visible on the surface of the pure epoxy coating (control) after 24 h exposure. In contrast, a relatively higher fraction of dead cells was observed on the surface of GOWE-0.1 specimen (Figure 5d). As the exposure continued to 96 h, the living cells with green fluorescence still dominated on the surface of the pure epoxy coating (Figure 5b), while dead (red) cells accounted for a large proportion on the surface of GOWE-0.1 coatings (Figure 5e). Furthermore, it noteworthy that healthy biofilms were formed on the surface of the pure epoxy coating. In comparison, biofilms on the surface of GOWE-0.1 coating were built up by loosely attached cells, which could be easily peeled off from the surface due to large number of dead cells and, therefore, less production of EPS (extracellular polymeric substance) secretion that can make the biofilm sticky ⁴¹. This result showed the beneficial addition of Graphene oxide to the epoxy to alleviate biofilm growth. As the exposure time continued to 10 days, almost all living (green) cells were still on the surface of the control coating (Figure 5c). Whereas almost all cells were dead (red) on the surface of the GOWE-0.1 coating (Figure 5f), which clearly demonstrated the sustainable ability of this coating to prevent biofilm formation.

After the antibacterial performance test, the coating samples were cleaned by sonication and DI water to be further analyzed to investigate the surface morphology through SEM. From the SEM images in Figure 6, there were no significant surface damages

and accumulated corrosion products on the surface of the GOWE-0.1 coating during the 10 days testing, while rough surface and unremoved accumulated products were easily observed on the surface of the pure epoxy coating.

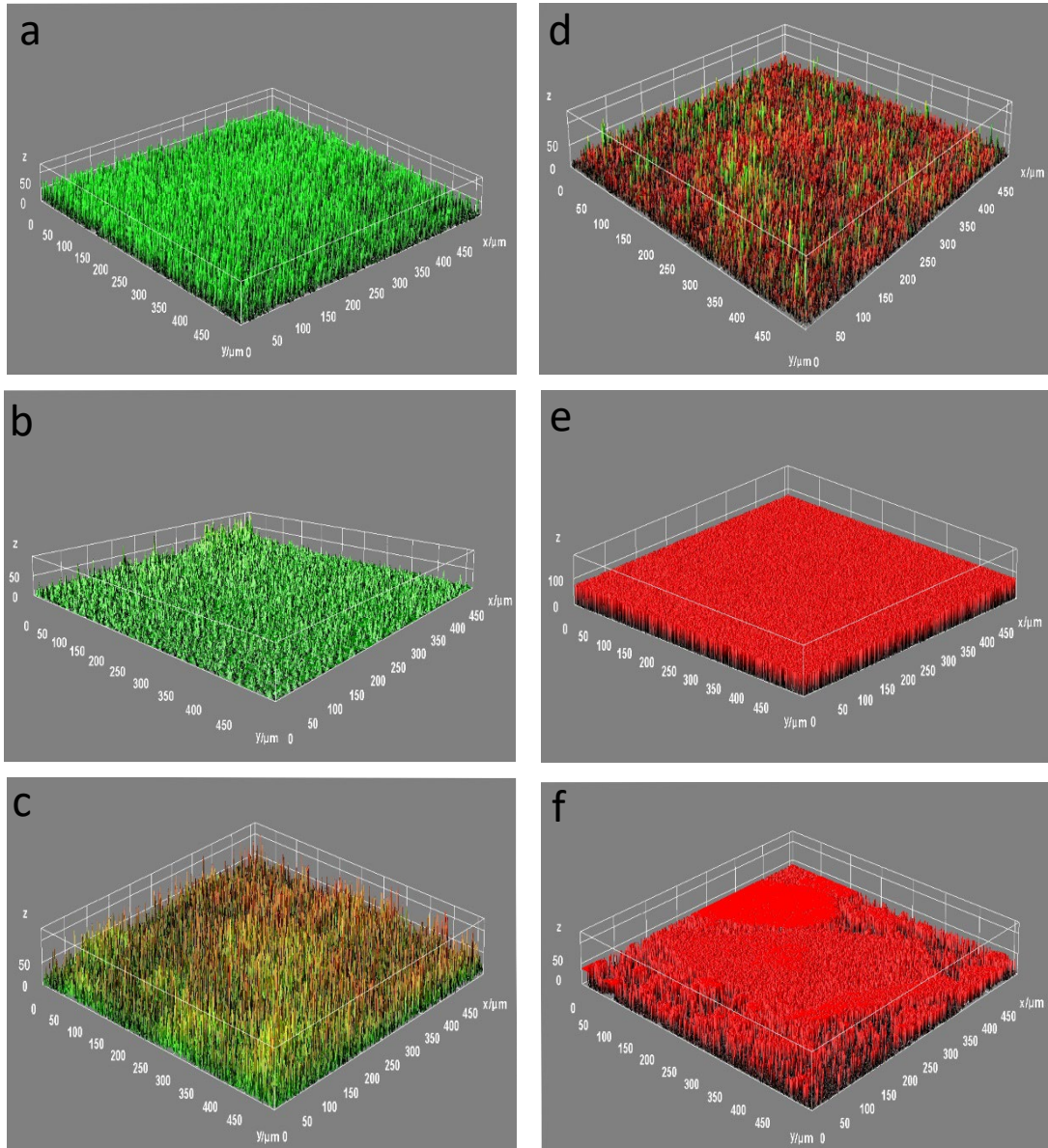


Figure 5. CLSM images of biofilms grown for (a) 24 h, (b) 96 h, and (c) 10 days for the WEP coating (control) and (d) 24 h, (e) 96 h, and (f) 10 days for GOWE-0.1 coating. The coating was

stained with SYTO9 and PI prior to microscopic observation. The red color corresponds to dead bacterial cells and the green color corresponds to living bacterial cells. The scale is in microns.

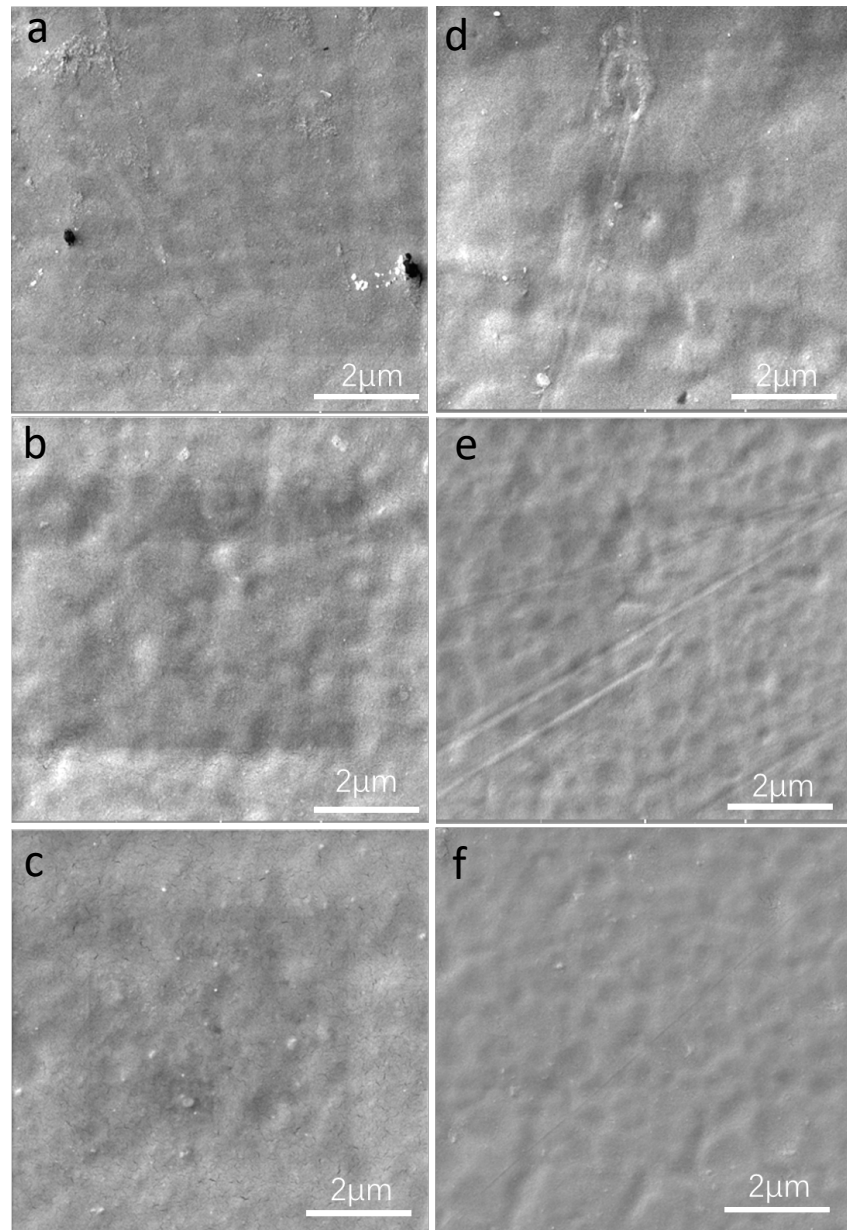


Figure 6. Surface morphology of WEP coating (control) and GOWE-0.1 coating (0.1 wt.% GO) after the exposure in *S. oneidensis* culture for a) 24 h, control b) 96 h, control and c) 10 days, control; d) 24 h, GOWE- 0.1 coating; e) 96 h, GOWE-0.1 coating and f) 10 days, GOWE-0.1 coating.

3.3. Effects of biofilm formation on anticorrosive performance of the GOWE coating

In this study, *Shewanella oneidensis* MR-1, a facultative metallic-reducing bacterium with metabolic versatility including aerobic respiration and dissimilatory Fe (III) reduction, was employed as a Fe (III) reduction bacterium (IRB) model since it can be found under steel corrosion conditions⁴². The influence of Fe reduction bacteria on corrosion performance remains controversial. Recent literature reviews have demonstrated that the effects of *Shewanella sp.* biofilm on corrosion behavior of a material can be negative or positive, highly dependent on the specific environmental factors, such as aerobic or anoxic (anaerobic) conditions, the presence of different electron acceptors, associated metabolic activities and metabolic versatility⁴³⁻⁴⁶. For example, Faisal et al. discovered that *Shewanella oneidensis sp.*, could inhibit corrosion of X52 carbon steel through iron respiration⁷. Contrarily, more recently, Li et al. reported *Shewanella sp.* could accelerate uniform or pitting corosions via bioanodic (biocathodic) EET (extracellular electron transfer)^{44,47}. Similarly, Miller et al. reported *S. oneidensis* MR-1 promoted corrosion under nitrate reducing conditions.⁴⁸

Therefore, understanding how *Shewanella sp.* contributes to the material corrosion is important since multiple environmental factors could synergistically promote or inhibit corrosion. Another aspect to be considered is the fact that most approaches for the protection of electrochemical corrosion and biofilm mediated corrosion has been developed by using nano patterning and surface treatment, which can resist bacterial attachment⁴⁹, thus efficiently impeding short-range electron transfers between bacteria and substrates. However, from this angle, the actual effects of *Shewanella oneidensis* MR-1 on

the composite polymeric coating, such as epoxy coating are still rarely reported. Hence, in this context, the real effects of the *Shewanella oneidensis* MR-1 on corrosion was also investigated in this experiment.

Specifically, to study the influence of biofilm formation on the anticorrosive performance of the GOWE coatings, the GOWE-0.1 coating samples with and without biofilm were evaluated by EIS measurement for 14 days. Figure 7 shows the impedance modulus at 0.01 Hz as a function of the immersion time for the control and GOWE-01 coated samples. Results show that the coating without bacteria exhibited better corrosion protection than the coating with the bacteria. This fact clearly demonstrated that the biofilm formed on the coating surface would accelerate the corrosion. This results also supported the previous study that *S. oneidensis* could accelerate the corrosion progress of Graphene oxide composite films under relative anaerobic conditions ⁵⁰. Although our experiments were not done in strictly anaerobic conditions, the fact that we did not mix constantly the media with the cells to well-aerate the growth media, could have generated a microaerophilic and anoxic condition on the surface of the coupons that were at the bottom of the wells. This could have explained the corrosive effects with the *S. oneidensis* and the additional presence of salt in the growth medium.

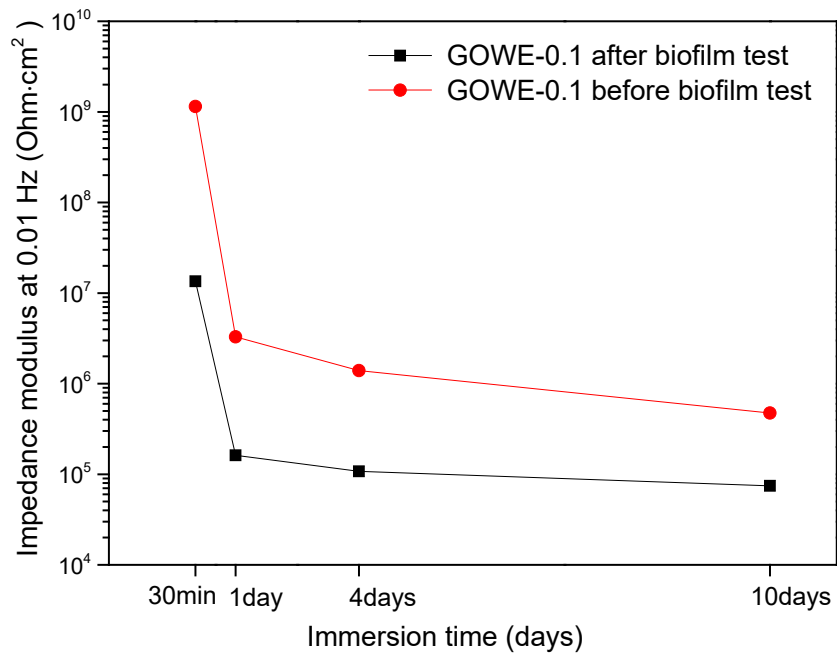


Figure 7. Impedance modulus at 0.01 Hz as a function of the immersion time for GOWE-0.1 coatings with and without biofilm testing.

3.4. Characterization of the best GOWE coating

3.4.1 Two-dimensional (2D) Graphene oxide nanolayer characterization

The morphological image of the as prepared Graphene oxide with the modified Hummers method is shown in Fig. 8a. A sheet-like two dimensional nanolayer structure was observed. The sharp edges and small few layers can be seen clearly. Fig. 8b indicated the XRD patterns of the raw material graphite and the synthesized Graphene oxide. A sharp diffraction peak of pure graphite was present at $2\theta = 26^\circ$ (002 plane), which corresponds to the graphite characteristic 002 plane (PDF No: 41-1487) and is consistent with previous research⁵¹. For the Graphene oxide, the broader peak at $2\theta = 10.7^\circ$ was observed, which

was assigned to (001) diffraction peak due to chemical oxidation action. This result was very close to the reported value in the literature, and this suggested the successful synthesis of Graphene oxide. Meanwhile, the disappearance of graphite (002) plane further proved that the complete oxidation of Graphene oxide occurred after the chemical exfoliation⁵².

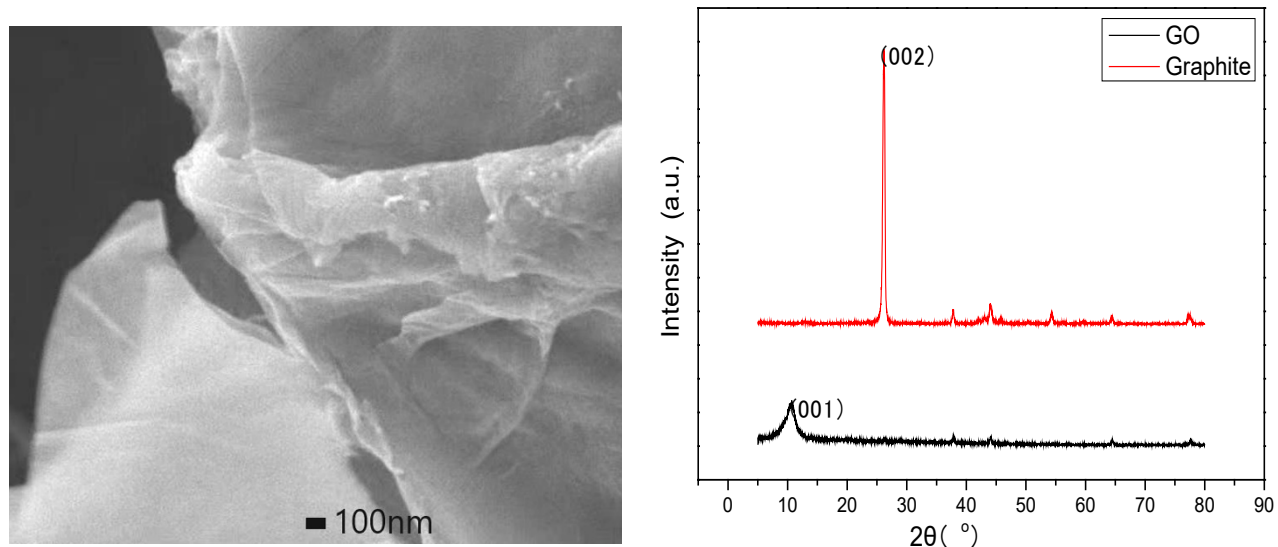


Figure 8 SEM image and XRD patterns of Graphene oxide.

3.4.2 Optimal GOWE coating characterization

The coatings prior to the analyses were characterized. Here, we report the characterization results of the optimum Graphene oxide concentration in the waterborne epoxy coating, which was determined to be 0.1 wt.% from the above-mentioned anticorrosive and antibacterial study. Therefore, the GOWE-0.1 coating film was characterized by Fourier transform infrared (FTIR) and Raman spectroscopy. The FTIR spectra of WEP (waterborne epoxy), GO (Graphene oxide), and GOWE-0.1 (0.1 wt.% GO)

coatings are shown in Figure 9. The typical characteristic peaks of GO (blue curve in Figure 9) were observed at 1735 cm^{-1} (C = O stretching vibration of – COOH groups), 3600 cm^{-1} (O – H stretching vibrations), 1095 cm^{-1} (C – O – C stretching vibration), 1260 cm^{-1} (– COH stretching), 1408 cm^{-1} (tertiary C – OH stretching vibration), 1018 and 1636 cm^{-1} (C = C stretching), and 2968 cm^{-1} (– CH stretching), which are in good agreement with the previously reported Graphene oxide spectrum ⁵³⁻⁵⁸. Further, the spectrum of waterborne epoxy (red curve in Figure 9) showed the typical characteristic IR band at 944 cm^{-1} (epoxide ring vibrations). Other representative groups of the epoxy resin include 1037 cm^{-1} , 1240 and 1110 cm^{-1} (symmetrical aromatic and aliphatic C – O stretch), 1183 , 1296 , and 1377 cm^{-1} (tertiary C – OH stretching vibration), 1458 cm^{-1} (deformation of C – H of CH₂/CH₃), 1503 and 1608 cm^{-1} (C = C of aromatic rings /C – C skeletal stretching), and 2878 , 2928 cm^{-1} (stretching C – H of CH₂ and C – H aromatic and aliphatic), which confirm the characteristic bands of key functional groups in the epoxy matrix ⁵⁹. For GOWE-0.1 coating (green curve in Figure 9), similar absorption bands were observed compared to the waterborne epoxy, especially in the region between $900 \sim 1600\text{ cm}^{-1}$ due to the relatively low content of Graphene oxide in the epoxy matrix. A distinct new band was found in the GOWE-0.1 coating, which was not observed in the pure epoxy and assigned to the characteristic absorption peaks of Graphene oxide at 1735 cm^{-1} , which clearly showed a C = O bond for the carboxyl group due to the existence of Graphene oxide. However, it is obvious that the intensity of the carboxyl groups (1735 cm^{-1}) became weaker and hydroxyl groups (– OH, 3600 cm^{-1}) disappeared when combining Graphene oxide with the epoxy matrix. This indicates that some reactions might have occurred between the carboxyl and hydroxyl groups of the Graphene oxide with the curing agent during the curing process ⁶⁰.

⁶². As a result, a three dimensional Graphene oxide network structure was formed in the waterborne epoxy matrix ⁶³.

The Raman spectrum of GOWE-0.1 (0.1 wt.% Graphene oxide) film is shown in Figure 10. The peak of GO at 1590 cm⁻¹ displayed the G-band, which corresponds to E2g phonon of sp² carbon-carbon bond and isolated double bonds on Graphene oxide sheets ⁶⁴. D-band appeared at 1355 cm⁻¹, which is characteristic of the graphene tangential vibrational mode (the breathing modes of six-membered rings activated by defects) ⁶⁵. These Raman peaks for **Graphene oxide** agree well with those reported previously by others ⁶⁶⁻⁶⁸. The ratio of the intensity of the D and G bands (ID/IG) of GOWE - 0.1 coating was approximately 0.89 by integrating the areas of D and G peaks. This was aligned with the typical **Graphene oxide** value obtained through oxidization and exfoliation of graphite as described in previous reports ^{69,70}, which demonstrated a good dispersion of the **Graphene oxide** nanofillers in the waterborne epoxy matrix. Other Raman peaks located at 1012, 1156, 1709, 2639, and 2759 cm⁻¹ are assigned to the vibrations of the epoxy ⁷⁰.

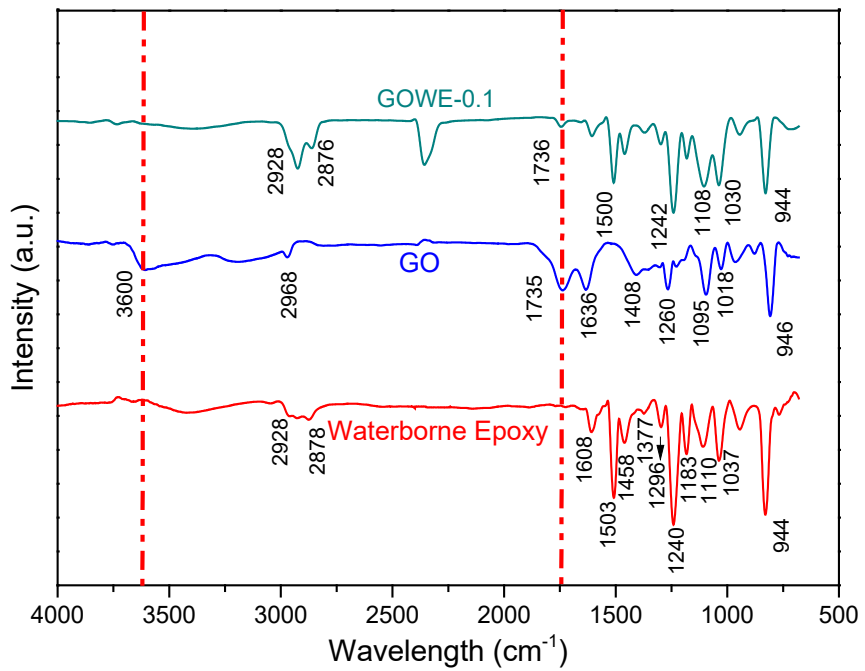


Figure 9. Fourier transform infrared spectra of GO, waterborne epoxy (control), and GOWE-0.1.

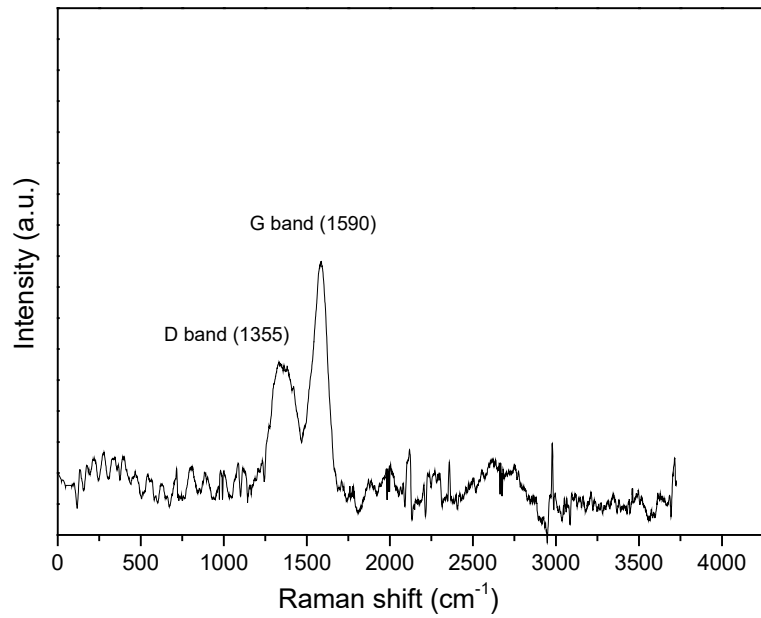


Figure 10. Raman spectra of the GOWE-0.1 coating.

3.5. Corrosion protection mechanism of the prepared coating

The anticorrosive enhancement of Graphene oxide-hybridized coating can be schematically illustrated in Figure 11. To understand the anticorrosive mechanism by Graphene oxide nanofillers, the coating surface was cut 2 cm in length by a blade for both WEP coating and GOWE-0.1 coating to simulate the accelerated local corrosion defects. The coated samples were firstly immersed in salt solution (8 wt.% NaCl) for 120 h. The images of the surfaces for waterborne epoxy coating with and without Graphene oxide after immersion are shown in Figure 11. After 120h testing, WEP control (Figure 11a) clearly showed serious local corrosion that demonstrated the corrosion agents (e.g. Cl⁻, O₂ and H₂O) had penetrated through the interface of the epoxy/metal and hydrolytically destroyed the coating, which caused the pit corrosion⁷¹. Furthermore, these pits near the crack regions on the coating could connect to each other first followed by the occurrence of spalling (Figure 11a).

On the other hand, there was no obvious corrosion defects on the surface of the GOWE-0.1 coating. In fact, the optimal GO content (0.1 wt.%) was assumed to form a homogeneous three-dimensional network structure, according to the above analysis (section 3.3, 3.4), by which could prevent local corrosion and significantly retard the propagation of the defects within the network structure. Additionally, the better coating adhesion achieved by incorporating well-dispersed Graphene oxide nanoplates in the epoxy allowed improved corrosive protection by the coating⁷². Additionally, electrons from iron oxidation in the micro-anode region can migrate through conductive nanoparticles, such as graphene oxide, which can alleviate the oxidation-reduction reaction

of corroded areas ⁷³. As a result, the prepared composite coating exhibited better corrosion protection as compared to the waterborne epoxy control (Figure 11), which was mainly attributed to the built three-dimensional network structure with well dispersed Graphene oxide.

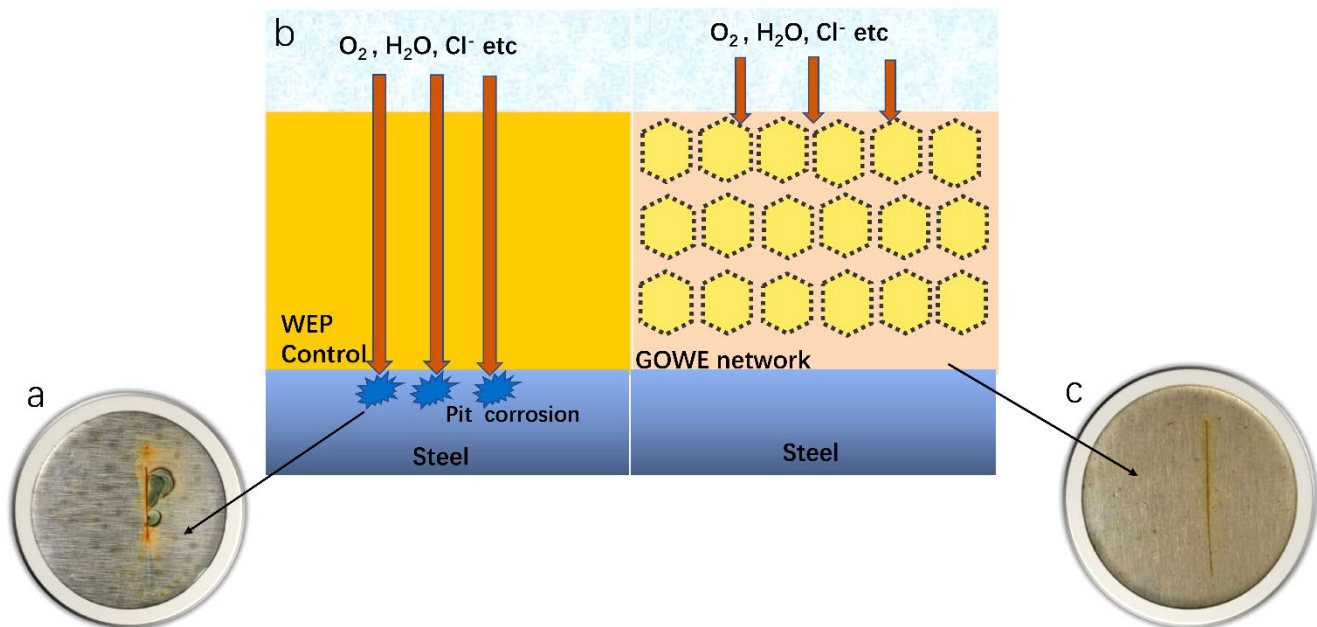


Figure 11. Surface morphology of WEP coating (control, without GO) and GOWE-0.1 (0.1 wt.% GO) before and after the exposure in 8 wt.% NaCl solution. a) WEP coating 120 h; c) GOWE-0.1 coating, 120 h; b) Schematic diagrams of the anticorrosive mechanism of WEP coating and the GOWE coating.

4. Conclusion

In this study, an effective **graphene oxide** hybridized waterborne epoxy coating was successfully developed as a coating material. The best concentration of Graphene oxide as nanofiller was identified to be 0.1 wt% for simultaneous anticorrosive and antibacterial protection of steel. The protection of steel was observed for more than 60 days for both 3.5% NaCl and against *S. oniedensis* MR-1. The protection against *S. oniedensis* MR-1 against corrosion was probably due to the biofilm inhibition observed in the coated material, since non coated material and the materials lacking graphene oxide presented the establishment of a biofilm and corrosion. Therefore, the newly developed **graphene oxide** hybridized waterborne epoxy coating can be potentially employed for applications that require simultaneous enhancement of anticorrosive and antibacterial functions.

Acknowledgement

The authors would like to acknowledge the following funding sources: Qatar National Research Foundation, award number: NPRP 9-318-1-064, the Robert A. Welch Foundation, 293 USA award number (E-2011-20190330), and the National Science Foundation under Grant No. CHE-1904472.

References

1. Fichman, G. *et al.* Seamless Metallic Coating and Surface Adhesion of Self-Assembled Bioinspired Nanostructures Based on Di-(3,4-dihydroxy-l-phenylalanine) Peptide Motif. *ACS Nano* **8**, 7220–7228 (2014).
2. Haute, D.V., LiuOrcid, A.T. & Orcid, J.M.B. Coating Metal Nanoparticle Surfaces with Small Organic Molecules Can Reduce Nonspecific Cell. *ACS Nano* **12**, 117–127 (2018).
3. Nguyen, H.N., Nadres, E.T., Alamani, B.G. & Rodrigues, D.F. Designing Polymeric Adhesives for Antimicrobial Materials: Poly(ethylene imine) Polymer, Graphene, Graphene Oxide and Molybdenum Trioxide - A biomimetic Approach. *Journal of Materials Chemistry B* **5**(2017).
4. Koch, G.H., J. Varney, N., Thompson, O., Moghissi, M.G. & Payer., J. International measures of prevention, application, and economics of corrosion technologies study. *NACE International*. (2016, Houston, HO, USA, .).
5. H. L. Lim. Assessing level and effectiveness of corrosion education in the UAE. *International Journal of Corrosion*. **2012**, 785701 (2012).
6. Mallakpour, S., Azadi, E. & Hussain., C.M. Recent breakthroughs of antibacterial and antiviral protective polymeric materials during COVID-19 pandemic and after pandemic: Coating, packaging, and textile applications. *Current Opinion in Colloid & Interface Science*. **55**(2021).
7. AlAbbas, F.M., Bhola, S. M., Spear, J. R., Olson, D. L. & Mishra, B. The shielding effect of wild type iron reducing bacterial flora on the corrosion of linepipe steel. . *Eng. Fail Anal.* **33**, 222–235 (2013).
8. Lekbach, Y. *et al.* Catechin hydrate as an eco-friendly biocorrosion inhibitor for 304L stainless steel with dual-action antibacterial properties against *Pseudomonas aeruginosa* biofilm. *Corrosion Science* **157**, 98-108 (2019).
9. Chopra, D., Gulati, K. & Ivanovski., S. Understanding and optimizing the antibacterial functions of anodized nano-engineered titanium implants. *Acta Biomaterialia* **127**, 80–101 (2021).
10. Zhang, S., Liang, X., Gaddc, G.M. & Zhao, Q. A sol–gel based silver nanoparticle/polytetrafluoroethylene (AgNP/PTFE) coating with enhanced antibacterial and anti-corrosive properties. . *Applied Surface Science* **535**, 147675 (2021).
11. Nie, Y. *et al.* MXene-hybridized silane films for metal anticorrosion and antibacterial applications. *Applied Surface Science* **527**, 146915 (2020).
12. Meng, J. *et al.* Advances in metal–organic framework coatings: versatile synthesis and broad applications. *Chem. Soc. Rev.*, **49**, 3142-3186 (2020).
13. Li, J. *et al.* Water-based rust converter and its polymer composites for surface anticorrosion. *Colloids Surf. A* **537** 334-342 (2018).
14. M.Atta, A., O.Ezzat, A., M.El-Saeed, A., M.Tawfeek, A. & I.Sabeela, N. Self-healing of chemically bonded hybrid silica/epoxy for steel coating. *Progress in Organic Coatings* **141**, 105549 (2020).
15. G. Christopher, M.A.K., G. Harichandran, . Comparative study of effect of corrosion on mild steel with waterborne polyurethane dispersion containing graphene oxide versus carbon black nanocomposites. *Prog. Org. Coat.* **89**, 199-211 (2015).
16. Nematollahi, M. *et al.* Comparison between the effect of nanoglass flake and montmorillonite organoclay on corrosion performance of epoxy coating,. *Corros.Sci.* **52**, 1809–1817 (2010).

17. Meng, F. *et al.* The influence of the chemically bonded interface between fillers and binder on the failure behaviour of an epoxy coating under marine alternating hydrostatic pressure, *. Corros. Sci.* **101**, 139–154 (2015).
18. Yadav, P.S., Purohit, R. & Kothari, A. Study of friction and wear behaviour of epoxy/nano SiO₂ based polymer matrix composites-A review. *Mater. Today. Proceed.* **18**, 5530–5539 (2019).
19. Georgakilas, V., Perman, J.A., Tucek, J. & Zboril., R. Broad family of carbon nanoallotropes: classification, chemistry, and applications of fullerenes, carbon dots, nanotubes, graphene, nanodiamonds, and combined superstructures. *Chemical Reviews* **115** 4744–4822 (2015).
20. Compton, O.C. *et al.* Chemically active reduced graphene oxide with tunable C/O ratios. *ACS Nano* **5**, 4380–4391 (2011).
21. Geim, A.K. & Novoselov., K.S. The rise of graphene, Nanoscience and Technology: A Collection of Reviews from Nature Journals,. *World Scientific.*, 11–19 (2010).
22. Ding, R. *et al.* Study on graphene modified organic anti-corrosion coatings: A comprehensive review. *Journal of Alloys and Compounds* **806**, 611-635 (2019).
23. Yu, Y.-H., Lin, Y.-Y., Lin, C.-H., Chana, C.-C. & Huang, Y.-C. Polym. Chem. . *High-performance polystyrene/graphene-based nanocomposites with excellent anti-corrosion properties.* **5**, 535-550 (2014).
24. Liu, Y. *et al.* Antibacterial graphene oxide coatings on polymer substrate. *Applied Surface Science* **436**, 624-630 (2018).
25. Fan, J., Grande, C.D. & Rodrigues, D.F. Biodegradation of graphene oxide-polymer nanocomposite films in wastewater. *Environmental science. Nano.* **4**(2017).
26. Peña-Bahamonde, J., San-Miguel, V., Cabanelas, J.C. & Rodrigues., D.F. Biological degradation and biostability of nanocomposites based on polysulfone with different concentrations of reduced graphene oxide. *Macromol. Mater. Eng.* **303** 1700359 (2018).
27. Hu, W. *et al.* Graphene-based antibacterial paper. *ACS Nano* **4**, 4317–4323 (2010).
28. Mirmohsenia, A., Azizia, M. & Dorraji, M.S.S. Facile synthesis of copper/ reduced single layer graphene oxide as a multifunctional nanohybrid for simultaneous enhancement of antibacterial and antistatic properties of waterborne polyurethane coating. *Progress in Organic Coatings* **131**, 322-332 (2019).
29. Ning, Y.-J., Zhu, Z.-R., Cao, W.-W., Wu, L. & Jing., L.-C. Anti-corrosion reinforcement of waterborne polyurethane coating with polymerized graphene oxide by the one-pot method. *Journal of Materials Science* **56**, 337–350 (2021).
30. J. Zhang *et al.* Dark, infrared reflective, and superhydrophobic coatings by waterborne resins. *Langmuir* **34**, 5600–5605 (2018).
31. Chen, C. *et al.* Bio-inspired superior barrier self-healing coating: Self-assemble of graphene oxide and polydopamine-coated halloysite nanotubes for enhancing corrosion resistance of waterborne epoxy coating. *Progress in Organic Coatings* **139**, 13 (2020).
32. Wang, N., Gao, H., Zhang, J. & Kang., P. Effect of Graphene Oxide/ZSM-5 Hybrid on Corrosion Resistance of Waterborne Epoxy Coating. **8**, 179 (2018).
33. Glasauer, S., Langley, S. & Beveridge., T.J. Intracellular iron minerals in a dissimilatory iron-reducing bacterium. *Science* **295**, 117-119 (2002).
34. Hang, N.N.E., T.N.; Bryan. G.A.; Debora, F.R. . Designing polymeric adhesives for antimicrobial materials: Poly(ethylene imine) polymer, graphene, graphene oxide and molybdenum trioxide-a biomimetic approach. *J. Mater. Chem. B* **28**, 6616–6628 (2017).

35. Ansari, A., Peña-Bahamonde, J., Wang, M. & Rodrigues., D.F. Polyacrylic acid-brushes tethered to graphene oxide membrane coating for scaling and biofouling mitigation on reverse osmosis membranes. *Journal of Membrane Science* **630**, 119308 (2021).

36. Wang, H.Z., Q. . Evaluation and failure analysis of linseed oil encapsulated self-healing anticorrosive coating. *Progress in Organic Coatings* **118**, 108-115 (2018).

37. Zhou, Q. & Wang, Y. Comparisons of clear coating degradation in NaCl solution and pure water. *Progress in Organic Coatings*. **76**, 1674-1682 (2013).

38. Pourhashem, S. *et al.* Polymer/Inorganic nanocomposite coatings with superior corrosion protection performance: A review. *Chemistry* **88**, 29-57 (2020).

39. Thormann, K.M., Saville, R.e.M., Shukla, S., Pelletier, D.A. & Spormann., A.M. Initial Phases of Biofilm Formation in *Shewanella oneidensis* MR-1. *Journal of bacteriology* **186**, 8096–8104 (2004).

40. Makabenta, J.M.V., Nabawy, A. & Li, C. Nanomaterial-based therapeutics for antibiotic-resistant bacterial infections. . *Nat Rev Microbiol.* **19**, 23–36 (2021).

41. Flemming, H., Wingender, J., Szewzyk, U. . Biofilms: an emergent form of bacterial life. *Nat Rev Microbiol.* **14**, 563–575 (2016).

42. Nina Wurzlera, J.D.S., Ralph Wagner, Matthias Dimper. Abundance of Fe(III) during cultivation affects the microbiologically influenced corrosion (MIC) behaviour of iron reducing bacteria *Shewanella Putrefaciens*. *Corrosion Science* **174**, 108855 (2020).

43. Bertling, K., Banerjee, A. & Saffarini, D. Aerobic Respiration and Its Regulation in the Metal Reducer *Shewanella oneidensis*. *Front Microbiol.* **12**, 723835 (2020).

44. Jiang, Z., Shi, M. & Shi, L. Degradation of organic contaminants and steel corrosion by the dissimilatory metal-reducing microorganisms *Shewanella* and *Geobacter* spp. *International biodeterioration & biodegradation* **147**, 104842.

45. Li, Z., Chang, W., Cui, T. & Xu, D. MR-1 bacteria could corrode steels via bioanodic or biocathodic EET in adaptation to the passive or active state of the steel surface. . *Communications materials* **2**(2021).

46. Miller, R.B., Sadek, A. & Rodriguez., A. Use of an Electrochemical Split Cell Technique to Evaluate the Influence of *Shewanella oneidensis* Activities on Corrosion of Carbon Steel. . *PLoS One* **11**, 147899 (2016).

47. Li, Z., Chang, W., Cui, T. & Xu, D. MR-1 bacteria could corrode steels via bioanodic or biocathodic EET in adaptation to the passive or active state of the steel surface. *Communications materials* **2**(2021).

48. Miller, R.B. *et al.* Use of an Electrochemical Split Cell Technique to Evaluate the Influence of *Shewanella oneidensis* Activities on Corrosion of Carbon Steel. *PLoS One* **11**, e0147899 (2016).

49. V.Singhal., A., DeepikaMalwal. & Thiagar., S. Antimicrobial and antibiofilm activity of GNP-Tannic Acid-Ag nanocomposite and their epoxy-based coatings. *Progress in Organic Coatings*. **159**, 106421 (2021).

50. Lou, Y. *et al.* Microbiologically influenced corrosion inhibition mechanisms in corrosion protection: A review. *Bioelectrochemistr* **141**, 107883 (2021).

51. Li, J., Zeng, X., Ren, T. & Van der Heide, E. The preparation of graphene oxide and its derivatives and their application in bio-tribological systems. *Lubricants* **2**, 137-161 (2014).

52. Paulchamy, B., Arthi, G. & and Lignesh, B.D. A simple approach to stepwise synthesis of graphene oxide nanomaterial, . *J. Nanomed. Nanotechnol.* **6**, 2–5 (2015).

53. A. Ensafi, A., Noroozi, R., Zandi, N. & AtashbarB. Rezaei. Cerium (IV) oxide decorated on reduced graphene oxide, a selective and sensitive electrochemical sensor for fenitrothion determination. . *Sensors and Actuators B: Chemical* **245**, 980-987 (2017).

54. Daniel R. Dreyer, S.P., Christopher W. Bielawski and Rodney S. Ruoff. The chemistry of graphene oxide. . *Chem. Soc. Rev.* **39**, 228-240 (2010).

55. Harfouche., N.G., N. . Electrodeposition of composite films of reduced graphene oxide/ polyaniline in neutral aqueous solution on inert and oxidizable metal. . *Journal of Electroanalytical Chemistry* **786**, 135–144 (2017).

56. Ma, Y., Di, H., Yu, Z. & Liang., L. Fabrication of silica-decorated graphene oxide nanohybrids and the properties of composite epoxy coatings research. *Applied surface science* **360**, 936-945 (2016).

57. Paredes, J., I. V.-R., S., Martinez-Alonso, A. & Tascon, J.M.D. *Langmuir* **24**, 10560-10564 (2008).

58. Shen, J.e.a. One Step Synthesis of Graphene Oxide-Magnetic Nanoparticle Composite. *J. Phys. Chem. C* (2010).

59. Huitao Yu, B.Z., Chaoke Bulin, Ruihong Li & Ruiguang Xing. High-efficient Synthesis of Graphene Oxide Based on Improved Hummers Method *Scientific reports*.

60. Vryonis, O., Virtanen, S.T.H. & Andritsch, T. Understanding the cross-linking reactions in highly oxidized graphene/epoxy nanocomposite systems. *J Mater Sci* **54**, 3035–3051 (2019).

61. Chauhana, D.S., Quraishia, M.A., Ansaria, K.R. & Salehb, T.A. One-step surface modification of graphene oxide and influence of its particle size on the properties of graphene oxide/epoxy resin nanocomposites. *European Polymer Journal* **101**, 211-217 (2018).

62. Ding, J., Zhao, H., Zhou, M., Liu, P. & Yu., H. Super-anticorrosive inverse nacre-like graphene-epoxy composite coating. *Carbon* **181**, 204-211 (2021).

63. Her, S.C. & Zhang, K.C. Mode I fracture toughness of graphene reinforced nanocomposite. . *Nanomaterials* **11**, 1743 (2021).

64. Pan, Y., Wang, J., Zhao, x., Li, c. & Wang, D.Y. Interfacial growth of MOF-derived layered double hydroxide nanosheets on graphene slab towards fabrication of multifunctional epoxy nanocomposites. *Chemical Engineering Journal* **330**, 1222–1231 (2017).

65. Kudin, K.N. *et al. Nano Lett.* **8**, 36–41 (2007).

66. Azizighannad, S. & Somenath Mitra, S. Reduction of Graphene oxide (GO) and Its effects on Chemical and Colloidal Properties. *Scientific Reports* **8**, 10083 (2018).

67. Díaz, D.L., Holgado, M.L., Fierro, J.L.G. & Velázquez., M.M. Evolution of the Raman Spectrum with the Chemical Composition of Graphene Oxide. *J. Phys. Chem. C* **121**, 20489–20497 (2017).

68. Pan, Y., Wang, J., Zhao, x., Li, c. & Wang, D.Y. Interfacial growth of MOF-derived layered double hydroxide nanosheets on graphene slab towards fabrication of multifunctional epoxy nanocomposites. *Chemical Engineering Journal* **330**, 1222–1231 (2017).

69. Jhajhari, S.K. & Selvaraj, K. Non-templated ambient nanoperforation of graphene: A novel scalable process and its exploitation for energy and environmental applications. *Nanoscale* **0**, 1-8 (2015).

70. KN, K. *et al. Raman spectra of graphite oxide and functionalized graphene sheets. Nano Lett.* **8**, 36-41 (2008).

71. KC, C., MH, H., H, L. & MC, L. Room-temperature cured hydrophobic epoxy/graphene composites as corrosion inhibitor for cold-rolled steel. *Carbon* **66**, 144–153 (2014).

72. Pourhashem, S. Corrosion Science. *Exploring corrosion protection properties of solvent based epoxygraphene oxide nanocomposite coatings on mild steel.* **115**, 78-92 (2017).
73. Yu, D., Wen, S., Yang, J., Wang, J. & Y. Wu. RGO modified ZnAl-LDH as epoxy nanostructure filler: a novel synthetic approach to anticorrosive waterborne coating. *Surf. Coat. Technol.* **326** (2017).